Fabrication of a Multilayer X-Band Band-Pass Metasurface Using Liquid Metal

Arkadeep Mitra, Kevin Xu, *Graduate Student Member, IEEE*, Komlan Payne, *Graduate Student Member, IEEE*, Jun H. Choi, *Member, IEEE*, and Jeong-Bong Lee, *Senior Member, IEEE*

***Abstract*—Fabrication of a physically flexible multi-layer metasurface composed of gallium-based liquid metal encapsulated in polydimethylsiloxane (PDMS) is reported. The second-order bandpass frequency selective surface (FSS) operating in the X-band is comprised of two modified Jerusalem cross resonator layers separated by an aperture layer. The multi-layer spatial filter has a total thickness of 4.81 mm (λ_0/7.5). An inverse image mold of the FSS layer patterns is fabricated in silicon, and FSS patterned PDMS is replicated from the silicon mold. The FSS patterned PDMS is spray coated with liquid metal to fabricate a massive array of discrete conductor patterns in PDMS and subsequent encapsulation by an additional layer of PDMS. Multiple versions of the m × n metasurfaces have been fabricated and have been repeatedly tested for their bendability, stretchability, twistability, and foldability. The fabricated metasurface in a waveguide environment demonstrated a band-pass center frequency at 8.33 GHz which agreed well with the simulated frequency at 8.31 GHz.**

***Index Terms*—Liquid metal, spray, flexible, band-pass, metasurface, PDMS.**

I. Introduction

GALLIUM-BASED liquid metals (e.g. Galinstan) exhibit unique material properties (liquid phase at room temperature with high electrical and thermal conductivity) [1], which coupled with low toxicity [2], have been studied for various soft, flexible electronics [3]–[17] applications including metasurfaces [18]–[20]. Liquid metal has been incorporated previously into the interconnected unit cells of the metasurfaces embedded in polydimethylsiloxane (PDMS) by using the mechanism of microfluidic injection filling [18]–[20].

Recently we have explored the avenue of incorporating liquid metal in a massive array of discrete metasurface patterns

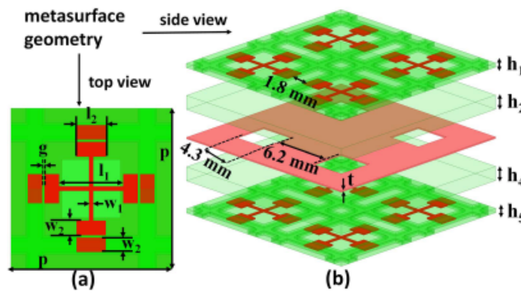

Fig. 1. Schematic diagram of the multi-layer band-pass metasurface: (a) Top view of a unit cell: $l_2 = 2$ mm, $l_1 = 4.3$ mm, $w_1 = 0.3$ mm, $w_2 = 1$ mm, $g = 0.2$ mm, $p = 10.5$ mm. (b) 3D view of 2 × 2 cells: $t = 0.2$ mm, $h_1 = 0.7$ mm, $h_2 = 1.66$ mm, $h_4 = 1.55$ mm, $h_5 = 0.7$ mm.

of unit cells incorporated in PDMS by using the mechanism of ultra-low pressure vacuum filling [21], [22]. However, such a mechanism might not be feasible for incorporating Galinstan in a multi-layer structure comprising of a continuous pattern situated in-between an array of discrete metasurface unit cell patterns. Moreover, the mechanism of vacuum filling depends on the expulsion of air completely from the microfluidic channels [23], [24], which increases the lag time (2-2.5 hours) from start to completion of filling of Galinstan in metasurface unit cells.

In this letter, we introduce the facile spray coating technique for incorporating Galinstan in continuous as well discrete unit cell patterns of a multi-layer metasurface. The physically flexible (stretchable, bendable, twistable, and foldable) multi-layer frequency selective surface (FSS) using Galinstan provides a second-order bandpass response in the X-band.

II. Design

The fabricated physically flexible multi-layer band-pass metasurface comprised of Galinstan ($t = 0.2$ mm) (Figure 1) encased within PDMS is a variation of a previously designed structure [25]. The PDMS layers in the top and bottom comprised of an m × n array of modified Galinstan-based Jerusalem cross frequency selective surface (FSS). The horizontal and vertical dipoles of the cross had 300 μm width, 4.3 mm length loaded with an end cap of 1 mm × 2 mm which faced the floating patches of the same size (Figure 1a). The thin (total thickness $h = 4.81$ mm, $\lambda_0/7.5$, where λ_0 is free space wavelength at approximately 8.3 GHz) metasurface's

Manuscript received 12 July 2022; accepted 27 July 2022. Date of publication 1 August 2022; date of current version 26 August 2022. This work was supported in part by the United States National Science Foundation under Grant NSF ECCS-1908779. The review of this letter was arranged by Editor M. Tabib-Azar. *(Corresponding author: Jeong-Bong Lee.)*

Arkadeep Mitra and Jeong-Bong Lee are with the Department of Electrical and Computer Engineering, University of Texas at Dallas, Richardson, TX 75080 USA (e-mail: jblee@utdallas.edu).

Kevin Xu and Jun H. Choi are with the Department of Electrical Engineering, University at Buffalo, Buffalo, NY 14260 USA.

Komlan Payne is with the Department of Biomedical Engineering, State University of New York at Buffalo, Buffalo, NY 14260 USA.

Color versions of one or more figures in this letter are available at https://doi.org/10.1109/LED.2022.3195323.

Digital Object Identifier 10.1109/LED.2022.3195323

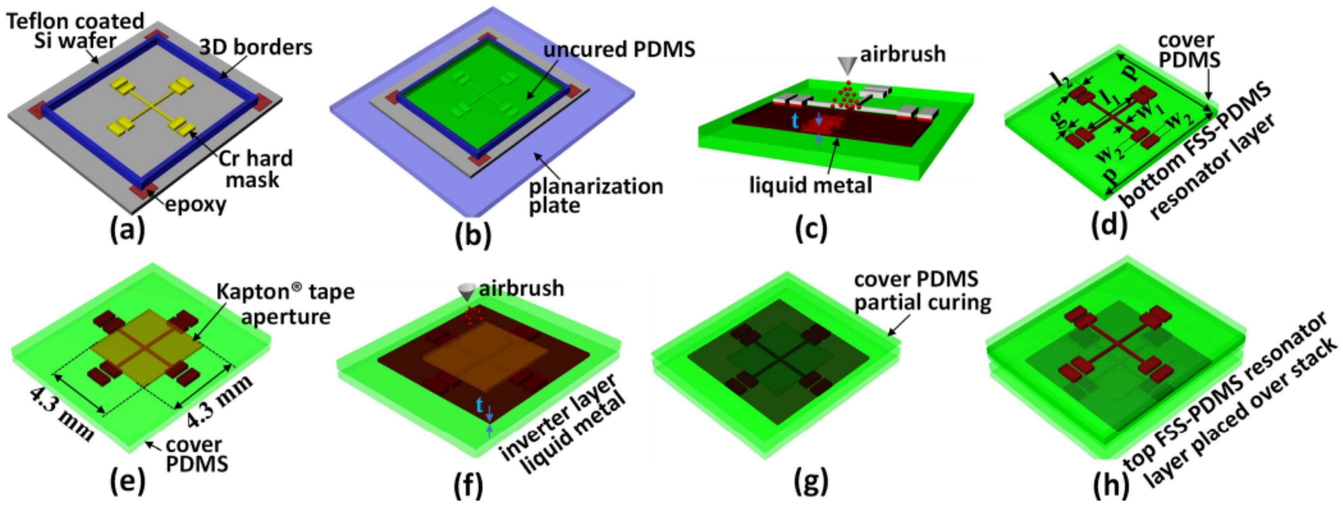

Fig. 2. Fabrication sequence of band-pass metasurface: (a) Dry-etched Si resonator mold. (b) Bottom FSS-PDMS resonator mold planarization. (c) Galinstan spraying using airbrush on replicated bottom FSS-PDMS resonator mold (t = 0.2 mm). (d) Cover PDMS for encapsulation of resonator mold, (e) Kapton® tape aperture placed overlapping the liquid metal patterned dipoles of modified Jerusalem cross. (f) Inverter layer liquid metal spraying using airbrush (t = 0.2 mm). (g) Partial curing of cover PDMS over the inverter layer, (h) liquid metal patterned dipoles of the top FSS-PDMS resonator mold aligned and bonded with bottom FSS-PDMS resonator mold.

layerwise substrate thickness is shown in Figure 1b. The multi-layer metasurface comprised of an inverter layer (square apertures: 4.3 mm × 4.3 mm) (Figure 1b) in the middle inductively coupling the horizontal and vertical dipoles of the Jerusalem cross FSS resonator layers. The metasurface was simulated in ANSYS HFSS.

III. Fabrication

Fabrication was started with patterning of S1813 photoresist (Micro Resist Technology) on a 4-inch silicon wafer and subsequent Cr layer deposition by e-beam evaporation and liftoff to get the patterned Cr layer for the modified Jerusalem cross resonator layers. Si was etched 0.2 mm using in inductively coupled plasma (ICP) with C_4F_8 (75 sccm), SF_6 (100 sccm), Ar (30 sccm) to create a mold. The patterned Si mold was coated with C_4F_8 (75 sccm) to have a 2 nm Teflon layer to ensure reliable replication.

3D printed borders were attached to the Si mold to facilitate PDMS curing (Figure 2a). The Si-mold was placed on a planarization plate and PDMS was casted over the mold as per designed thickness (Figure 2b). Planarization was allowed at room temperature for 24 hours. After planarization, thermal curing of the bottom FSS-PDMS resonator mold was done on a hotplate (96° C) for 21 minutes. After curing Galinstan (Ga 68.5%, In 21.5%, Sn 10%) was sprayed into the patterns using airbrush (36 psi) (Figure 2c). Following cleaning of the excess liquid metal outside of patterns, PDMS was casted again and cured at room temperature for 48 hours to encapsulate the patterned liquid metal in the modified Jerusalem cross resonator (Figure 2d).

Four layers of Kapton® tape (DuPont, Wilmington, DE, USA) (thickness: 55 μm/layer) were stacked and cut in shape of square apertures measuring 4.3 mm × 4.3 mm. The Kapton® tape square apertures were placed overlapping the liquid metal patterned horizontal and vertical dipoles

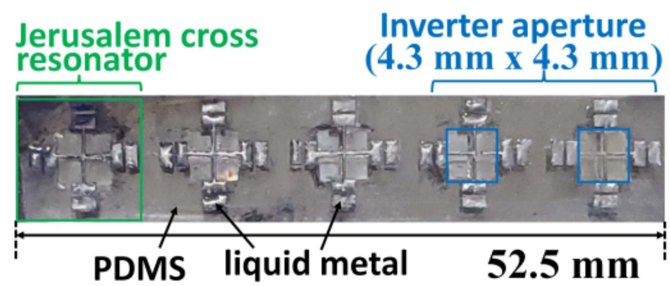

Fig. 3. A photomicrograph of 1 × 5 fabricated band-pass metasurface.

of the bottom FSS-PDMS resonator mold, by flipping over the liquid metal patterned modified Jerusalem cross with cover PDMS (Figure 2e). Galinstan was sprayed to form the inverter layer by using an airbrush (Figure 2f). Followed by spraying and liquid metal planarization, the Kapton® tape square apertures were peeled off and PDMS was casted again to cover the inverter layer. The cover PDMS of the inverter layer was allowed to partially cure at room temperature for 22 hours (Figure 2g).

The liquid metal patterned top FSS-PDMS resonator mold was fabricated following the fabrication steps of the bottom FSS-PDMS resonator. At the end of 22 hours of partial curing, the horizontal/vertical dipole alignment of the liquid metal patterned modified Jerusalem cross of the top FSS-PDMS resonator mold was done with respect to the bottom FSS resonator mold before placement over the collective stack. Curing of the integrated multi-layer structure (h = 4.81 mm) was done for 48 hours at room temperature (Figure 2h).

Multiple band-pass metasurfaces of m × n array were fabricated. Figure 3 shows a top view of a 1 × 5 metasurface. Multiple metasurfaces were repeatedly tested for their physical flexibility; namely, bendability, stretchability, twistability, and foldability (Figure 4). However, no visually identifiable

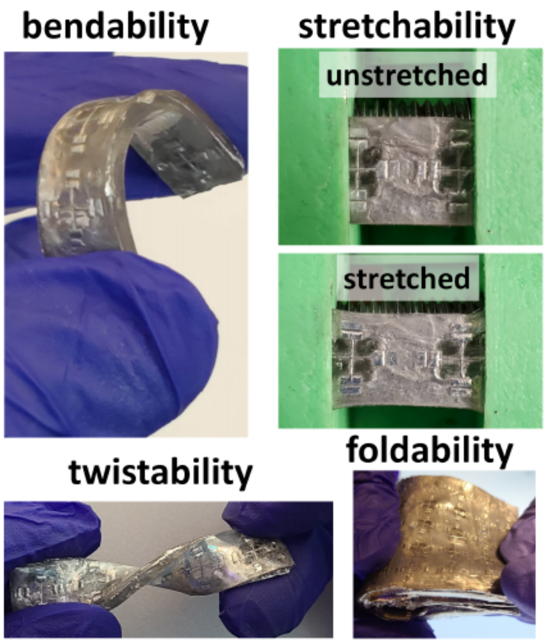

Fig. 4. Physical flexibility demonstration of the fabricated metasurface.

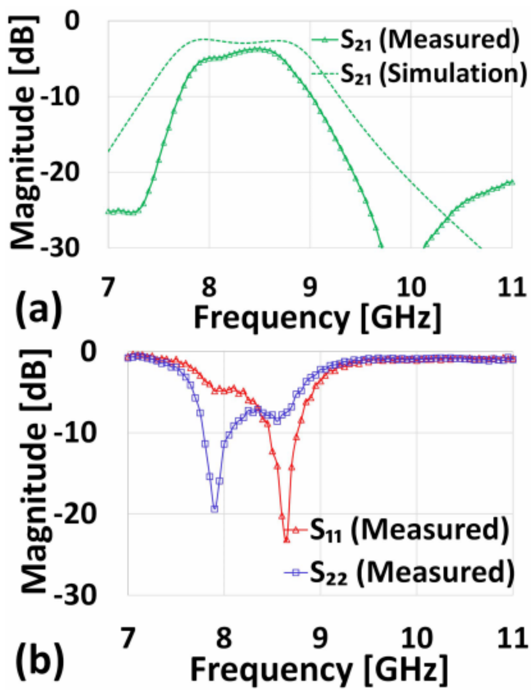

Fig. 5. WR-90 waveguide results for band-pass metasurface. (a) Simulated and measured transmission coefficient. (b) Measured reflection coefficients.

damage was on the metasurface after more than 20 cycles, demonstrating its physical flexibility.

IV. Characterization

A 1 × 2 metasurface cut from a fabricated 1 × 5 metasurface was characterized inside WR-90 waveguide. Detailed measurement setup has been previously described [21], [22]. The measured S-parameter results for the reflection and transmission of the multi-layer metasurface show good agreement with the simulated results (Fig. 5). The center frequency of the simulated and measured sample was observed at 8.31 GHz and 8.33 GHz, with a 3-dB fractional bandwidth of 17% and 12% respectively (Fig. 5a).

V. Conclusion

Eliminating the need of a previously reported sophisticated vacuum system [21], [22], Galinstan was spray coated using an airbrush in continuous as well as discrete patterns (t = 0.2 mm) encapsulated in multiple PDMS layers enabling extremely thin (h = 4.81 mm) high-order band-pass metasurface operating in the X-band (7 - 11.2 GHz) by the virtue of inverter coupling. The simulated band-pass center frequency at 8.31 GHz showed good agreement with the measured center frequency at 8.33 GHz. The demonstration of physically flexible (bendable, stretchable, twistable, and foldable) band-pass metasurface may enable transportable, conformable, and field deployable metasurfaces uniquely suited for practical applications in restricted volume in space and military applications..

References

[1] T. Daeneke, K. Khoshmanesh, N. Mahmood, I. A. de Castro, D. Esrafilzadeh, S. J. Barrow, M. D. Dickey, and K. Kalantarzadeh, "Liquid metals: Fundamentals and applications in chemistry," *Chem. Soc. Rev.*, vol. 47, no. 11, pp. 4073–4111, Apr. 2018, doi: 10.1039/C7CS00043J.

[2] Y. Lu, Q. Hu, Y. Lin, D. B. Pacardo, C. Wang, W. Sun, F. S. Ligler, M. D. Dickey, and Z. Gu, "Transformable liquid-metal nanomedicine," *Nature Commun.*, vol. 6, no. 1, pp. 1–10, Dec. 2015, doi: 10.1038/NCOMMS10066.

[3] Y. Wang, Y. Lu, D. Mei, and L. Zhu, "Liquid metal-based wearable tactile sensor for both temperature and contact force sensing," *IEEE Sensors J.*, vol. 21, no. 2, pp. 1694–1703, Jan. 2021, doi: 10.1109/JSEN.2020.3015949.

[4] T. Liu, P. Sen, and C.-J. Kim, "Characterization of liquid-metal Galinstan for droplet applications," in *Proc. IEEE 23rd Int. Conf. Micro Electro Mech. Syst. (MEMS)*, Jan. 2010, pp. 560–563, doi: 10.1109/MEMSYS.2010.5442440.

[5] K. Mohseni and E. S. Baird, "Digitized heat transfer using electrowetting on dielectric," *Nanosc. Microscale Thermophys. Eng.*, vol. 11, nos. 1–2, pp. 99–108, May 2007, doi: 10.1080/15567260701337555.

[6] S. W. Jin, J. Park, S. Y. Hong, H. Park, Y. R. Jeong, J. Park, S.-S. Lee, and J. S. Ha, "Stretchable loudspeaker using liquid metal microchannel," *Sci. Rep.*, vol. 5, no. 1, pp. 1–13, Jul. 2015, doi: 10.1038/SREP11695.

[7] A. Tabatabai, A. Fassler, C. Usiak, and C. Majidi, "Liquid-phase gallium–indium alloy electronics with microcontact printing," *Langmuir*, vol. 29, no. 20, pp. 6194–6200, May 2013, doi: 10.1021/LA401245D.

[8] L. Ren, J. Zhuang, G. Casillas, H. Feng, Y. Liu, X. Xu, Y. Liu, J. Chen, Y. Du, L. Jiang, and S. X. Dou, "Nanodroplets for stretchable superconducting circuits," *Adv. Funct. Mater.*, vol. 26, no. 44, pp. 8111–8118, Nov. 2016, doi: 10.1002/ADFM.201603427.

[9] R. Guo, X. Wang, W. Yu, J. Tang, and J. Liu, "A highly conductive and stretchable wearable liquid metal electronic skin for long-term conformable health monitoring," *Sci. China Technol. Sci.*, vol. 61, no. 7, pp. 1031–1037, Jul. 2018, doi: 10.1007/S11431-018-9253-9.

[10] Y. Wu, Y. Zhou, W. Asghar, Y. Liu, F. Li, D. Sun, C. Hu, Z. Wu, J. Shang, Z. Yu, R.-W. Li, and H. Yang, "Liquid metal-based strain sensor with ultralow detection limit for human–machine interface applications," *Adv. Intell. Syst.*, vol. 3, no. 10, May 2021, Art. no. 2000235, doi: 10.1002/AISY.202000235.

[11] E. J. Markvicka, M. D. Bartlett, X. Huang, and C. Majidi, "An autonomously electrically self-healing liquid metal-elastomer composite for robust soft-matter robotics and electronics," *Nature Mater.*, vol. 17, no. 7, pp. 618–624, May 2018, doi: 10.1038/S41563-018-0084-7.

[12] S. I. Rich, R. J. Wood, and C. Majidi, "Untethered soft robotics," *Nature Electron.*, vol. 1, no. 2, pp. 102–112, Feb. 2018, doi: 10.1038/S41928-018-0024-1.

[13] G. Li, X. Wu, and D.-W. Lee, "A galinstan-based inkjet printing system for highly stretchable electronics with self-healing capability," *Lab Chip*, vol. 16, no. 8, pp. 1366–1373, Mar. 2016, doi: 10.1039/C6LC00046K.

[14] Y. Lin, C. Cooper, M. Wang, J. J. Adams, J. Genzer, and M. D. Dickey, "Handwritten, soft circuit boards and antennas using liquid metal nanoparticles," *Small*, vol. 11, no. 48, pp. 6397–6403, Nov. 2015, doi: 10.1002/SMLL.201502692.

[15] D. Kim, D. Jung, J. H. Yoo, Y. Lee, W. Choi, G. S. Lee, K. Yoo, and J.-B. Lee, "Stretchable and bendable carbon nanotube on PDMS super-lyophobic sheet for liquid metal manipulation," *J. Micromech. Microeng.*, vol. 24, no. 5, Apr. 2014, Art. no. 055018, doi: 10.1088/0960-1317/24/5/055018.

[16] W. Tang, T. Jiang, F. R. Fan, A. F. Yu, C. Zhang, X. Cao, and Z. L. Wang, "Liquid-metal electrode for high-performance triboelectric nanogenerator at an instantaneous energy conversion efficiency of 70.6%," *Adv. Funct. Mater.*, vol. 25, no. 24, pp. 3718–3725, May 2015, doi: 10.1002/ADFM.201501331.

[17] D. Kim, Y. Lee, D.-W. Lee, W. Choi, K. Yoo, and J.-B. Lee, "Hydrochloric acid-impregnated paper for gallium-based liquid metal microfluidics," *Sens. Actuators B, Chem.*, vol. 207, pp. 199–205, Feb. 2015, doi: 10.1016/j.snb.2014.09.108.

[18] S. Ghosh and S. Lim, "Fluidically reconfigurable multifunctional frequency-selective surface with miniaturization characteristic," *IEEE Trans. Microw. Theory Techn.*, vol. 66, no. 8, pp. 3857–3865, Aug. 2018, doi: 10.1109/TMTT.2018.2829195.

[19] H. K. Kim, D. Lee, and S. Lim, "Wideband-switchable metamaterial absorber using injected liquid metal," *Sci. Rep.*, vol. 6, no. 1, pp. 1–11, Aug. 2016, doi: 10.1038/SREP31823.

[20] K. Ling, K. Kim, and S. Lim, "Flexible liquid metal-filled metamaterial absorber on polydimethylsiloxane (PDMS)," *Opt. Exp.*, vol. 23, no. 16, pp. 21375–21383, Aug. 2015, doi: 10.1364/OE.23.021375.

[21] A. Mitra, K. Xu, S. Babu, J. H. Choi, and J. Lee, "Liquid-metal-enabled flexible metasurface with self-healing characteristics," *Adv. Mater. Interfaces*, vol. 9, no. 12, Apr. 2022, Art. no. 2102141, doi: 10.1002/ADMI.202102141.

[22] A. Mitra, K. Xu, S. Babu, J. H. Choi, and J.-B. Lee, "Liquid metal-based flexible band-stop frequency selective surface," in *Proc. IEEE 34th Int. Conf. Micro Electro Mech. Syst. (MEMS)*, Gainesville, FL, USA, Jan. 2021, pp. 953–956, doi: 10.1109/MEMS51782.2021.9375361.

[23] Y. Lin, O. Gordon, M. R. Khan, N. Vasquez, J. Genzer, and M. D. Dickey, "Vacuum filling of complex microchannels with liquid metal," *Lab Chip*, vol. 17, no. 18, pp. 3043–3050, Aug. 2017, doi: 10.1039/C7LC00426E.

[24] J. Monahan, A. A. Gewirth, and R. G. Nuzzo, "A method for filling complex polymeric microfluidic devices and arrays," *Anal. Chem.*, vol. 73, no. 13, pp. 3193–3197, May 2001, doi: 10.1021/AC001426Z.

[25] K. Xu, J. H. Choi, K. Payne, J. K. Lee, and J.-B. Lee, "Flexible liquid metal frequency selective surface with tunable second-order bandpass response," in *Proc. IEEE Int. Symp. Antennas Propag. North Amer. Radio Sci. Meeting*, Jul. 2020, pp. 725–726, doi: 10.1109/IEEECONF35879.2020.9330077.